Desalination and Water Treatment
www.deswater.com

doi: 10.5004/dwt.2019.23172

142 (2019) 167–178
February

Optimization of Fe^{2+} catalyzed hydrogen peroxide/persulfate and its application in activated carbon regeneration

Shengpin Li[a,b], Wenpeng Li[a], Boyang Liu[b], Fei Liu[b,*], Honghan Chen[b], Xiulan Yin[a], Song Jin[c,d], Yi Li[e], Zaixing Huang[c], Michael A. Urynowicz[c]

[a]*China Institute of Geo-Environment Monitoring, Beijing 100081, China, Tel. +86-10-62172031; emails: shengpin1988@163.com (S. Li), liwp@mail.cigem.gov.cn (W. Li), yinxl@mail.cigem.gov.cn (X. Yin)*
[b]*Beijing Key Laboratory of Water Resources and Environmental Engineering, China University of Geosciences, Beijing 100083, China, Tel. +86-151-20086112; Fax: +86-010-82321081; email: feiliu@cugb.edu.cn (F. Liu), Tel. +86-10-82321027; emails: 1820304783@qq.com (B. Liu), chenhh56@126.com (H. Chen)*
[c]*Department of Civil and Architectural Engineering, University of Wyoming, 1000 East University Avenue, Laramie, WY 82071, United States, Tel. +1-307-766-4398; emails: sjin@uwyo.edu (S. Jin), zhuang@uwyo.edu (Z. Huang), murynowi@uwyo.edu (M.A. Urynowicz)*
[d]*Advanced Environmental Technologies LLC, 4025 Automation Way, Suite F4, Fort Collins, CO 80525, United States*
[e]*Geological Environmental Monitoring Station of Hebei Province, Shijiazhuang 050021, China, Tel. +86-13933129093; email: 13933129093@163.com*

Received 24 April 2018; Accepted 17 September 2018

ABSTRACT

Activated carbon (AC) is widely used in the removal of organic contaminants; however, its long-term use is impeded by the limited adsorption capacity. Regeneration of AC by using advanced oxidation has been in practice, especially for Fe^{2+}/H_2O_2 process and $Fe^{2+}/S_2O_8^{2-}$ process, however, both of them have limitations in the regeneration of AC. This work attempted the combination of Fe^{2+}/H_2O_2 and $Fe^{2+}/S_2O_8^{2-}$ ($Fe^{2+}/H_2O_2/S_2O_8^{2-}$) to effectively regenerate AC and recover its activity through exposing fresh carbon on its surface. Trichloroethylene (TCE) was selected as the target contaminant in this study. Fe^{2+}, H_2O_2, and $S_2O_8^{2-}$ were the variables to optimize for AC's regeneration. Based on the variation of variables obtained from Fe^{2+}/H_2O_2 process and $Fe^{2+}/S_2O_8^{2-}$ process, the response surface methodology (RSM) was applied to have the optimum ratio of variables for the regeneration of AC of $Fe^{2+}/H_2O_2/S_2O_8^{2-}$ process. Results from RSM show that the $Fe^{2+}/H_2O_2/S_2O_8^{2-}$ process achieved a molar ratio of TCE/$Fe^{2+}/H_2O_2/S_2O_8^{2-}$ at 1/9.00/56.63/76.25. The iron loss was measured at 2.84%, while the TCE removal efficiency reached 98.63%. The average regeneration rate of AC through the optimized $Fe^{2+}/H_2O_2/S_2O_8^{2-}$ process was 26.28%, with minimum iron precipitation.

Keywords: Activated carbon; Regeneration; Fenton' reagent; Persulfate; Optimization; Response surface methodology

1. Introduction

Due to its high surface area and porous structure, activated carbon (AC) is widely used for organic contamination control [1]. Since it is an adsorbent, AC can physically adsorb gases and compounds that are dispersed or dissolved in liquids [2], especially for organic contaminants, however, the long-term use of AC is limited due to the significant reduction of adsorption capacity. Several methods have been studied for regeneration of AC saturated with organic contaminants. Advanced oxidation processes (AOPs) is one of the most promising methods to treat aqueous effluents containing

---

* Corresponding author.
Present address: Haiyang Mailbox, China University of Geosciences, Beijing. No.29 Xueyuan Road, Haidian District, Bejing 100083, PR China.

organic contaminants [2,3]. Regeneration of AC is possible through the AOPs, especially for Fenton and persulfate processes, which showed great potential as viable regeneration technologies for rapidly treating organic contaminants from AC [4,5]. Fenton's reagent involves the reaction between hydrogen peroxide (H_2O_2) and ferrous iron (Fe^{2+}) (Eqs. (1) and (2)), which forms the hydroxyl radical ($HO^{\bullet}$, $E^{\theta} = 2.7$ V), a powerful and nonspecific oxidation intermediate that can degrade many kinds of organic contaminant (s) of concern [6–9]. Yet, the conventional Fe^{2+}/H_2O_2 process in AC regeneration is limited by iron loss (iron precipitation) in the reaction process that can possibly affect the surface characters of AC. Besides, the optimum pH (~3) needs to be adjusted in Fe^{2+}/H_2O_2 process [10–12].

$$Fe^{2+} + H_2O_2 \rightarrow Fe^{3+} + HO^{\bullet} + OH^{-} \tag{1}$$

$$Fe^{3+} + H_2O_2 \rightarrow Fe^{2+} + HO_2^{\bullet} + H^{+} \tag{2}$$

Persulfate ($S_2O_8^{2-}$) possesses a high redox potential at 2.01 V and is relatively stable in the subsurface. Under certain reaction conditions (e.g., activated heat, Fe^{2+}, and UV), $S_2O_8^{2-}$ can generate a sulfate radical ($SO_4^{\bullet-}$, $E^{\theta} = 2.6$ V), which has a strong oxidizing ability [13–15] (Eqs. (3)–(5)). Moreover, an acidic pH in groundwater will be created by $S_2O_8^{2-}$ itself or $S_2O_8^{2-}$ reactants that consume alkalinity and generate hydrogen ion (Eqs. (4) and (5)). As a result, rapid elimination of target organic contaminants can be achieved through a $Fe^{2+}/S_2O_8^{2-}$ process [16,17], however, high dosages of Fe^{2+} are required, and residual Fe^{2+} can result in the consumption of $SO_4^{\bullet-}$ [18–21]. Therefore, it is necessary to optimize the Fe^{2+} amount that is used in the $Fe^{2+}/S_2O_8^{2-}$ process for AC regeneration.

$$S_2O_8^{2-} + \text{Heat or } Fe^{2+} \rightarrow SO_4^{\bullet-} + SO_4^{2-} + Fe^{3+} \tag{3}$$

$$SO_4^{\bullet-} + OH^{-} \rightarrow SO_4^{2-} + HO^{\bullet} \tag{4}$$

$$SO_4^{\bullet-} + H_2O \rightarrow SO_4^{2-} + HO^{\bullet} + H^{+} \tag{5}$$

Research has focused on the application of the Fe^{2+}/H_2O_2 process when combined with the $Fe^{2+}/S_2O_8^{2-}$ process (defined as the $Fe^{2+}/H_2O_2/S_2O_8^{2-}$ process) [22–24]. Fe^{2+} can be used as a catalyst for both H_2O_2 and $S_2O_8^{2-}$ to produce radicals in the $Fe^{2+}/H_2O_2/S_2O_8^{2-}$ process, therefore, Fe^{2+} can be used effectively to avoid excess Fe^{2+} consuming $SO_4^{\bullet-}$. Furthermore, the pH of the reaction environment dropped as a result of $S_2O_8^{2-}$, which would favor the reaction and bypass iron precipitation [10]. The results of the $Fe^{2+}/H_2O_2/S_2O_8^{2-}$ process were promising for the regeneration of AC, however, optimization of the process is still required to make it economically viable on an industrial scale.

The statistical design can be used to optimize the process through highly effective operating conditions and minimizing the number of experiments [25]. There is a particular interest in regard to response surface methodology (RSM). RSM is a mathematical tool that was statistically designed to describe the relation between independent variables and one or more responses, enabling process optimization with a reduced number of experimental trials [26,27].

In this work, the $Fe^{2+}/H_2O_2/S_2O_8^{2-}$ process was optimized for AC regeneration by RSM and trichloroethylene (TCE) was selected as the target contaminant. The significance of this study provides the feasibility of $Fe^{2+}/H_2O_2/S_2O_8^{2-}$ process in the regeneration of AC through the comparison of different AOPs regeneration methods. Furthermore, based on the composition of $Fe^{2+}/H_2O_2/S_2O_8^{2-}$ process, optimization of the oxidants ratios by RSM was conducted to reduce the oxidants dosages and get the optimal AC regeneration efficiency. The approach can be summarized as follows: the first part involved the evaluation of the Fe^{2+}/H_2O_2 process, $Fe^{2+}/S_2O_8^{2-}$ process and $Fe^{2+}/H_2O_2/S_2O_8^{2-}$ process for AC regeneration, which were used to evaluate the regeneration effect of AC by different oxidation processes. The second part was obtaining the variables used for RSM calculation, including different Fe^{2+}/H_2O_2 ratios in Fe^{2+}/H_2O_2 process that effect TCE removal and iron loss control, different $Fe^{2+}/S_2O_8^{2-}$ ratios in $Fe^{2+}/S_2O_8^{2-}$ process that effect TCE removal and pH. According to the level of variables obtained from the Fe^{2+}/H_2O_2 and $Fe^{2+}/S_2O_8^{2-}$ processes, RSM was applied to optimize the $Fe^{2+}/H_2O_2/S_2O_8^{2-}$ process. The final part was the evaluation in TCE removal, total iron loss control, $HO^{\bullet}$ generation, and AC regeneration efficiency for the most optimal $Fe^{2+}/H_2O_2/S_2O_8^{2-}$ process that could be obtained from RSM.

2. Materials and methods

2.1. Chemicals

All chemicals used in this study were prepared with ultrapure water from a Millipore system (USA). Granular AC (20–40 mesh) was purchased from Sigma-Aldrich (USA) that is used as the adsorbent for TCE. Trichloroethylene was the selected contaminant (C_2HCl_3, TCE ≥ 98%). Ferrous sulfate heptahydrate ($FeSO_4 \cdot 7H_2O$, ≥99%), hydrogen peroxide (H_2O_2, ≥30%), and sodium persulfate ($Na_2S_2O_8$, ≥98%) were used as oxidation system to regenerate saturated AC. Benzoic acid (C_6H_5COOH, ≥98%) was used as radical scavenger to capture $HO^{\bullet}$. *p*-Hydroxybenzoic acid ($C_7H_6O_3$, ≥98%) was the product of benzoic acid and $HO^{\bullet}$, which was used as a standard material for $HO^{\bullet}$ detection. H_2SO_4 and NaOH were used to adjust pH in the experiment. Ascorbic acid ($C_6H_8O_6$, ≥98%) was used to terminate the radical reactions during the regeneration process [28]. Chemicals were all analytical reagent grade and obtained from Beijing Chemical Works (Beijing, China).

2.2. Experiment design

All trials of the Fe^{2+}/H_2O_2, $Fe^{2+}/S_2O_8^{2-}$, and $Fe^{2+}/H_2O_2/S_2O_8^{2-}$ processes were performed in batch mode and in non-buffered solutions at ambient room temperature. The initial pH of samples was adjusted with H_2SO_4 (1 mol/L) and NaOH (1 mol/L). The initial regeneration pH of samples was adjusted to ~3 with H_2SO_4 (1mol/L), unless otherwise stated. All experiments were conducted in a 2 L conical flask with a teflon-coated plug and a magnetic stirring apparatus. The reaction liquid was stirred with a magnetic stirrer that had adjustable agitation rate (150 rpm). All experiments were performed with an initial volume of 2 L and an initial TCE concentration of 30 mg/L (0.229 mmol/L). The initial Fe^{2+}, H_2O_2, and $S_2O_8^{2-}$ concentrations during the experiments were based on the input TCE amount that is in a certain molar ratio. Experiments that involved controls were setup in triplicate (the TCE that escaped the system was accounted for in the mass balance). The ascorbic acid was used to terminate the radical reactions.

2.2.1. Evaluation of different oxidation processes in AC regeneration

In order to investigate the AC regeneration process, different oxidants concentrations were selected. The adsorption experiments were conducted in 2 L TCE solutions (30 mg/L) with 1 g AC. In the regeneration process of AC, the adsorption process was conducted first, while the solution pH was fixed at 7, the reaction time was selected for 12 h (according to the results from kinetic tests when the adsorption equilibrium was achieved). The adsorption processes were conducted three times to help AC saturate (not fully saturated), the saturated AC was then freeze-dried to help regenerate. During the regeneration process, based on the adsorbed TCE amount, Fe^{2+}/TCE (molar ratio) were set at 0.5, 1, 2, and 4. H_2O_2 and $S_2O_8^{2-}$ concentrations were set at H_2O_2/TCE = 20 (molar ratio), $S_2O_8^{2-}$/TCE = 1 (molar ratio). The surface characters of AC, TCE removal, and chloride ion were investigated during the regeneration.

In accordance to the optimized $Fe^{2+}/H_2O_2/S_2O_8^{2-}$ process, the regeneration experiments of AC were conducted. The adsorption and regeneration processes were the same as mentioned earlier, however, TCE/$Fe^{2+}/H_2O_2/S_2O_8^{2-}$ used in the regeneration was based on the optimized results (in molar ratio). The adsorption/regeneration cycle was repeated three times. During the regeneration, the TCE removal, chloride ion, $HO^\bullet$ generation, and the surface characters of AC were investigated.

The calculation of AC regeneration efficiency can be described as Eq. (6). TCE was finally oxidized to chloride during the regeneration (1 molar TCE can finally generate 3 molar chloride, no intermediates were detected during the regeneration), which means that chloride can represent the oxidized amount of TCE. The generated chloride divided by 3 was the oxidized TCE amount (in molar ratio).

$$\text{AC regeneration efficiency}(\%) = \frac{\text{Cl}^-_{\text{generation amount}}}{3 \times \text{TCE}_{\text{absorbed amount}}} \times 100 \quad (6)$$

2.2.2. Optimization of Fe^{2+}/H_2O_2 process and $Fe^{2+}/S_2O_8^{2-}$ process

To obtain the variables used for RSM from Fe^{2+}/H_2O_2 process, the molar ratio of TCE/H_2O_2/Fe^{2+} in 1/10/6, 1/20/1, 1/20/3, 1/20/6, 1/20/9, 1/20/12, 1/40/6, 1/40/9, 1/40/12, 1/60/6, 1/60/9, 1/60/12, and 1/60/15 were setup. As with $Fe^{2+}/S_2O_8^{2-}$ process, the molar ratio of TCE/$S_2O_8^{2-}$/Fe^{2+} in 1/40/3, 1/40/9, 1/40/12, 1/40/15, 1/60/6, 1/60/9, 1/60/12, 1/60/15, 1/80/9, 1/80/12, and 1/80/15 were conducted to obtain the variables used for RSM. The reaction time was set to 30 min based on our previous research that in 30 min the reaction was almost finished. An aliquot of 5 mL reaction solution was sampled with a 10 mL borosilicate vial containing 1 mL ascorbic acid (0.1 mol/L) at 5 min intervals. TCE and total iron concentrations were analyzed during the Fe^{2+}/H_2O_2 process, TCE concentrations and pH were analyzed during the $Fe^{2+}/S_2O_8^{2-}$ process.

2.2.3. Optimization of $Fe^{2+}/H_2O_2/S_2O_8^{2-}$ using RSM

The goal of RSM is to optimize the ratios of Fe^{2+}, H_2O_2, and $S_2O_8^{2-}$ in $Fe^{2+}/H_2O_2/S_2O_8^{2}$ process, which aimed to improve TCE removal efficiency and reduce total iron loss while reducing the surface destruction of AC during regeneration process. Based on the initial TCE concentration, Fe^{2+}, H_2O_2, and $S_2O_8^{2-}$ were calculated as Fe^{2+}/TCE, H_2O_2/TCE, and $S_2O_8^{2-}$/TCE (in molar ratio), which were referred as X_1, X_2, and X_3, respectively. The responses of TCE removal efficiency and the total iron concentration (the concentration of iron in solution, %) were referred to as Y_1 and Y_2, respectively. In accordance to Box–Behnken design principles, a 3-level-3-factor of 17 experimental points experiment was designed. The experiment data were processed by Design-Expert 8.0.6 software. The results of the RSM were evaluated for TCE removal, total iron loss, pH variation, and $HO^\bullet$ generation.

2.3. Analytical methods

TCE was analyzed by using an Agilent GC-6820 with a headspace autosampler (HP 7694E), a FID detector, and a 30 m × 0.53 mm DB-5 capillary column (film thickness 1.5 μm). Total iron ions (Fe) amounts were analyzed by ICP-OES (Spectroblue, Germany). The value of pH was determined by using a Sartorious PB-10 pH meter. In order to investigate the $HO^\bullet$ concentrations, benzoic acid was selected as the radical scavenger [29]. Benzoic acid and *p*-hydroxybenzoic acid were determined by using an Agilent 1220 HPLC that was equipped with a ZORBAX SB-Aq column (5 μm, 4.6 × 150 mm) and HPLC-UV detection at 240 nm. TCE was finally oxidized to chloride during the regeneration (1 molar TCE can generate 3 molar chloride), which means that chloride can present the oxidized amount of TCE. Chloride was determined by silver nitrate titration (0.01 mol/L) by using an automatic potentiometric titrator (Metrohm 877 Titrino plus equipped with Metrohm 801 stirrer, Switzerland). An S-4800 field emission scanning electron microscope (SEM; Hitachi, Japan) and an Escalab 250Xi X-ray photoelectron spectrometer (Thermo Scientific, USA) were used to assess the surface structure change of the AC. Pore size and volume were determined by using an ASAP2020 physical adsorption instrument (Micromeritics instrument corp, USA).

3. Results and discussion

3.1. Evaluation of different oxidation processes in AC regeneration

The results of the Fe^{2+}/H_2O_2, $Fe^{2+}/S_2O_8^{2-}$, and $Fe^{2+}/H_2O_2/S_2O_8^{2-}$ processes for AC regeneration are presented in Fig. 1. Because H_2O_2 and $S_2O_8^{2-}$ concentrations were fixed at H_2O_2/TCE = 20 (molar ratio) and $S_2O_8^{2-}$/TCE = 1 (molar ratio), respectively. With molar ratio of Fe^{2+}/TCE varied from 0.5 to 4, Fe^{2+}/TCE = 0.5 showed the highest TCE removal from AC, while Fe^{2+}/TCE = 4 showed the least TCE removal. In comparison with the Fe^{2+}/H_2O_2 and $Fe^{2+}/S_2O_8^{2-}$ processes, the $Fe^{2+}/H_2O_2/S_2O_8^{2-}$ process achieved the highest TCE removal from AC with the least Fe^{2+} dosages (Fe^{2+}/TCE = 0.5), indicating that in the $Fe^{2+}/H_2O_2/S_2O_8^{2-}$ process, Fe^{2+} can catalyze both H_2O_2 and $S_2O_8^{2-}$ to generate $HO^\bullet$ in the regeneration of AC.

With the Fe^{2+}/TCE ratios increasing, the removed TCE from AC decreased. The reason for this might be the surplus of Fe^{2+} in oxidation processes. The increased Fe^{2+}/TCE ratio resulted in more $HO^{\bullet}$ generation. However, the increased Fe^{2+} amount tend to result in a Fe^{2+} residual, which can consume $HO^{\bullet}$ in the oxidation process simultaneously [30]. Furthermore, iron precipitation will appear with high Fe^{2+}/TCE ratios, which can prevent the contact of $HO^{\bullet}$ with the adsorbed TCE on AC.

With molar ratio of the Fe^{2+}/TCE = 0.5, $Fe^{2+}/H_2O_2/S_2O_8^{2-}$ process showed a significant advantage in TCE removal (Fig. 1). However, with a molar ratio of Fe^{2+}/TCE = 1, 2, and 4, there was no significant difference among $Fe^{2+}/H_2O_2/S_2O_8^{2-}$ process, Fe^{2+}/H_2O_2 process, and $Fe^{2+}/S_2O_8^{2-}$ process. This indicated that the uncalculated Fe^{2+}, H_2O_2, and $S_2O_8^{2-}$ matching cannot fully utilize the advantages of the $Fe^{2+}/H_2O_2/S_2O_8^{2-}$ process, therefore, optimization of the process is required to make it more efficient for AC regeneration.

Furthermore, during the regeneration process the surface characters of AC were partly changed. This can be seen in the $Fe^{2+}/H_2O_2/S_2O_8^{2-}$ process (Fe^{2+}/TCE = 0.5) as presented in Figs. 2 and 3. As seen with the SEM, near 1 and 2 μm gray as well as iron precipitation appeared on the surface of AC after regeneration.

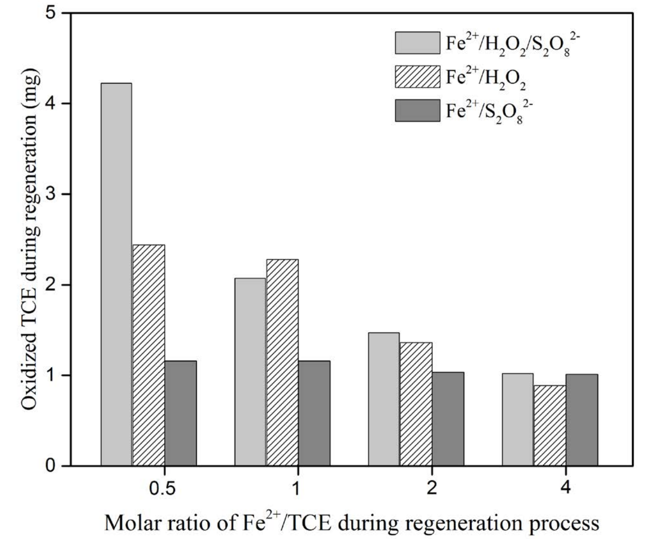

Fig. 1. Different oxidation processes in AC regeneration (molar ratio of Fe^{2+}/TCE were 0.5, 1, 2, and 4, respectively, H_2O_2/TCE = 20, $S_2O_8^{2-}$/TCE = 1. $[TCE]_0$ = 60 mg (0.458 mmol), initial pH of regeneration is 3).

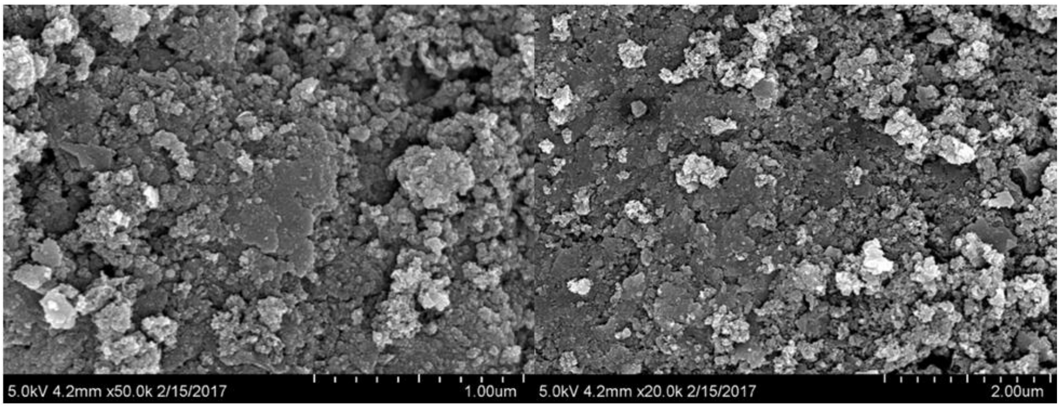

Fig. 2. AC surface before regeneration by $Fe^{2+}/H_2O_2/S_2O_8^{2-}$ process (with molar ratio of $Fe^{2+}/H_2O_2/S_2O_8^{2-}$/TCE = 0.5/20/1/1, $[TCE]_0$ = 60 mg (0.458 mmol), initial pH of regeneration is 3).

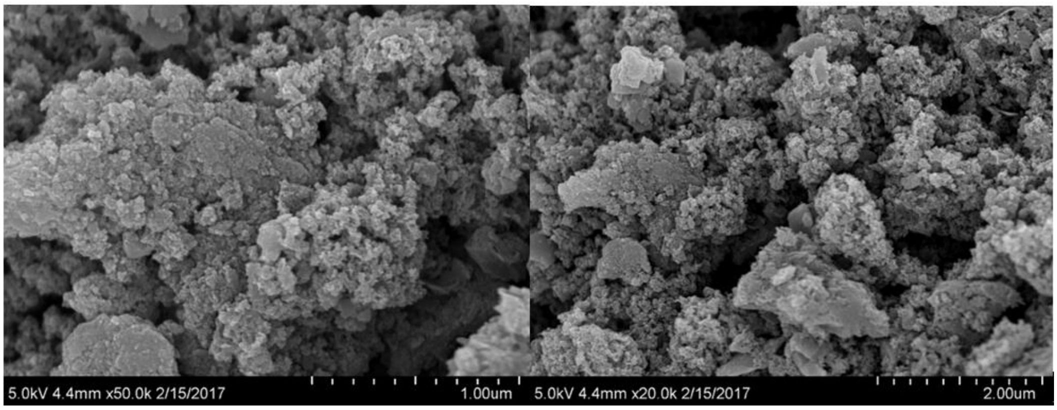

Fig. 3. AC surface after regeneration by $Fe^{2+}/H_2O_2/S_2O_8^{2-}$ process (with molar ratio of $Fe^{2+}/H_2O_2/S_2O_8^{2-}$/TCE = 0.5/20/1/1, $[TCE]_0$ = 60 mg (0.458 mmol), initial pH of regeneration is 3).

AC's surface area and pore volume played an important role in TCE adsorption, especially for recovering the activity of AC. As presented in Table 1, the BET surface area of the regenerated AC decreased 43.9% compared with the original AC, indicating that the regeneration process can reduce the AC's surface area and its adsorption capacity. The volume of pore size <0.47 nm increased after regeneration, which was attributed to the crash and erosion during the regeneration process. The total volume of pore size ≤216.63 nm decreased to 40.4%, while the total area in pores ≥0.47 nm decreased to 61.3%, leading us to infer that the crash and erosion during the regeneration process was mainly distributed in pore sizes ≥0.47 nm and ≤216.63 nm.

The initial elements of AC mainly contained C (81.88%), O (9.43%), and N (2.17%), the latter accounting for about 93.48% of the total AC weight. After regeneration, the content of C decreased from 81.88% to 55.69%, N decreased from 2.17% to undetected, while O increased from 9.43% to 22.36%. For Cl and Fe, the contents of them increased from 0.18% and 0.99% to 2.68% and 6.52%, respectively. The decrease of C content indicated that the surface and inner pores of AC were partly destroyed during the regeneration process, leading to a carbon loss. The adsorption capacity of AC is strongly unfavored by a high O content, however, the regeneration process resulted in a increase of O [31,32]. The increase of Cl content reflected the accumulation of TCE in AC, indicating that fully regeneration of AC cannot be achieved. The increase in Fe on the surface of AC suggested that there was iron precipitation formed during the regeneration process.

Table 1
Change of AC's surface character after regeneration by $Fe^{2+}/H_2O_2/S_2O_8^{2-}$ process (with molar ratio of $Fe^{2+}/H_2O_2/S_2O_8^{2-}/TCE$ = 0.5/20/1/1, $[TCE]_0$ = 60 mg (0.458 mmol), initial pH of regeneration is 3)

Category	Original AC	Regenerated AC
BET surface area (m^2/g)	647.88	363.49
Volume in pores <0.47 nm (cm^3/g)	0.02	0.04
Total volume in pores ≤216.63 nm (cm^3/g)	0.49	0.29
Total area in pores ≥0.47 nm (m^2/g)	463.76	179.52

A few studies showed that there was a positive relationship between C amounts and AC adsorption as well as a negative relationship between O and AC adsorption [31,32]. The loss of C and the increase of O decreased the AC adsorption capacity, which resulted in the reduction of TCE removal efficiency after regeneration.

It can be found that with a certain ratio of Fe^{2+}, H_2O_2, and $S_2O_8^{2-}$ during the AC regeneration process, though the regeneration efficiency of AC was acceptable, C content, AC surface area, and pores decreased, O content and iron precipitation increased, all of which displayed an adverse effect on the sustainable use of AC. The deterioration of AC in the regeneration process is inevitable, whatever physical or chemical methods. For $Fe^{2+}/H_2O_2/S_2O_8^{2-}$ process, the advantages were obvious, which can take advantage of both Fe^{2+}/H_2O_2 process and $Fe^{2+}/S_2O_8^{2-}$ process. However, it is necessary to optimize the $Fe^{2+}/H_2O_2/S_2O_8^{2-}$ process to have high TCE removal from AC, with less iron precipitation and AC deterioration.

3.2. Optimization of $Fe^{2+}/H_2O_2/S_2O_8^{2-}$ process

In accordance to RSM, three variables including Fe^{2+}, H_2O_2, and $S_2O_8^{2-}$ concentrations were evaluated and two responses including TCE removal efficiency and total iron concentrations (Fe^{2+} and Fe^{3+}, %) were assessed in the optimization of the $Fe^{2+}/H_2O_2/S_2O_8^{2-}$ process. In order to obtain the level of variables used in RSM, the Fe^{2+}/H_2O_2 and $S_2O_8^{2-}/Fe^{2+}$ processes were conducted at different Fe^{2+}, H_2O_2, and $S_2O_8^{2-}$ concentrations.

3.2.1. Optimization of Fe^{2+}/H_2O_2 process in TCE removal and total iron loss

The main goals of this study are the evaluation of the Fe^{2+}/H_2O_2 process in TCE removal, total iron loss control, and obtaining the variables used for RSM. The results of TCE oxidation by the classical Fe^{2+}/H_2O_2 process is presented in Fig. 4. As expected, the Fe^{2+}/H_2O_2 process demonstrated a high oxidation efficiency, resulting in TCE removal in less than 5 min, even at low oxidation concentrations of 1/20/1

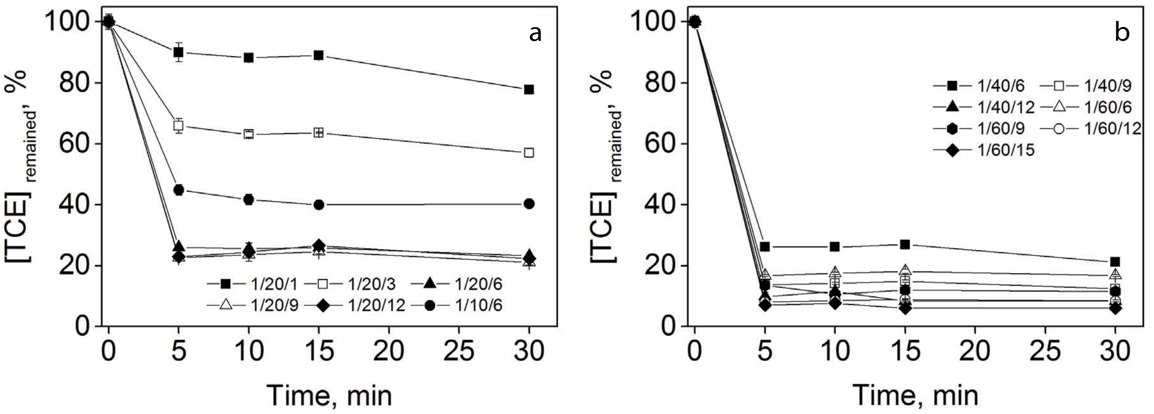

Fig. 4. Degradation of TCE by the $Fe^{2}/H_2O_2^{+}$ process ($TCE/H_2O_2/Fe^{2+}$ is a molar ratio, $[TCE]_0$ = 0.228 mmol/L).

($TCE/H_2O_2/Fe^{2+}$, m/m/m). A further increase in the oxidant dosage of H_2O_2 and Fe^{2+} led to higher TCE removal efficiency, in which the highest performance was achieved at $TCE/H_2O_2/Fe^{2+}$ concentrations of 1/60/15 with a TCE removal efficiency of 93.97%. The results also suggested that a certain threshold of the $TCE/H_2O_2/Fe^{2+}$ ratio (1/20/9, 1/20/12, 1/40/9, 1/20/12, 1/40/12, 1/60/9, 1/60/12, and 1/60/15) could lead to the desired high TCE removal efficiency. Based on TCE removal efficiency, the reasonable Fe^{2+}/TCE ratio parameters in RSM would be 9, 12, and 15. The suggested H_2O_2/TCE ratio parameters would be 20, 40, and 60.

The results indicated remarkable loss of total iron concentrations during the reaction even with an initial pH adjustment to 3, as shown in Table 2. The iron loss ranged from 17.42% to 27.64%. The ratio of oxidant and catalyst had a significant impact on the iron losses. For instance, with the increasing amounts of Fe^{2+} and H_2O_2 (1/60/9-1/60/15), the TCE removal efficiency increased from 88.45% to 93.97%. Coincidently, the iron loss increased concomitantly for the same respective ratio from 17.76% to 27.64%.

In general, the Fe^{2+}/H_2O_2 process proved to be an efficient technique for TCE degradation with a certain amount of Fe^{2+} input. However, the total iron loss increased as TCE removal efficiency increased, especially in groundwater remediation that the iron precipitation is easily effect the permeability of aquifers. It is necessary to reduce the iron usage and achieve a high TCE removal efficiency meantime.

Table 2
The total iron loss (Fe^{2+} and Fe^{3+}) in Fe^{2+}/H_2O_2 process ($TCE/H_2O_2/Fe^{2+}$ is a molar ratio, $[TCE]_0$ = 0.228 mmol/L, t = 30 min)

$TCE/H_2O_2/Fe^{2+}$, (m/m/m)	Initial Fe (mg/L)	Final Fe (mg/L)	Fe loss (%)	TCE removal (%)
1/20/9	131.28	104.2	20.63	78.96
1/20/12	175.18	133.29	23.91	77.70
1/40/9	126.81	104.72	17.42	87.60
1/40/12	172.75	133.41	22.77	91.60
1/60/9	125.41	103.14	17.76	88.45
1/60/12	169.76	124.19	26.84	91.55
1/60/15	211.68	153.18	27.64	93.97

3.2.2. *Optimization of TCE removal and pH variation in $Fe^{2+}/S_2O_8^{2-}$ process*

The performance of the $S_2O_8^{2-}/Fe^{2+}$ process in TCE removal and pH adjustment were studied at different $TCE/S_2O_8^{2-}/Fe^{2+}$ ratios. The effect of oxidant doses in TCE removal was evaluated and the results are presented in Fig. 5. A fast degradation of TCE was observed during the first 5 min, with TCE being gradually degraded within the remaining reaction time. With the Fe^{2+}/TCE ratio increasing from 3 to 15 (molar ratio) in the $TCE/S_2O_8^{2-}/Fe^{2+}$ of 1/40/3, 1/40/9, 1/40/12, 1/40/15, the TCE removal efficiency increased from 48.32% to 87.08%. A further increase in the oxidant dosage led to a higher TCE removal efficiency ($TCE/S_2O_8^{2-}/Fe^{2+}$ = 1/80/15, 90.67%). However, a significant amount of $S_2O_8^{2-}$ and Fe^{2+} were consumed in the process.

The results also suggested that a certain threshold of $TCE/S_2O_8^{2-}/Fe^{2+}$ ratio (1/40/9, 1/40/12, 1/40/15, 1/60/9, 1/60/12, 1/60/15, 1/80/9, 1/80/12, and 1/80/15) could lead to a high TCE removal efficiency. Based on TCE removal efficiency percentages, the reasonable Fe^{2+}/TCE ratio parameters in RSM would be 9, 12, and 15. The suggested $S_2O_8^{2-}$/TCE ratio parameters would be 40, 60, and 80. As shown in Table 3 the initial solution pH decreased from ~3 to below 3 (2.56–2.87) at 30 min with the addition of $S_2O_8^{2-}$, which means that

Table 3
The pH variation in $S_2O_8^{2-}/Fe^{2+}$ process ($TCE/S_2O_8^{2-}/Fe^{2+}$ is a molar ratio, $[TCE]_0$ = 0.228 mmol/L, t = 30 min)

$TCE/S_2O_8^{2-}/Fe^{2+}$ (m/m/m)	Initial pH	Final p.H	TCE removal (%)
1/40/9	3.03	2.87	73.33
1/40/12	3.02	2.67	55.30
1/40/15	3.01	2.56	86.08
1/60/9	3.04	2.83	72.05
1/60/12	3.02	2.72	78.62
1/60/15	3.03	2.68	81.62
1/80/9	3.03	2.82	85.21
1/80/12	3.01	2.72	81.72
1/80/15	3.03	2.63	90.67

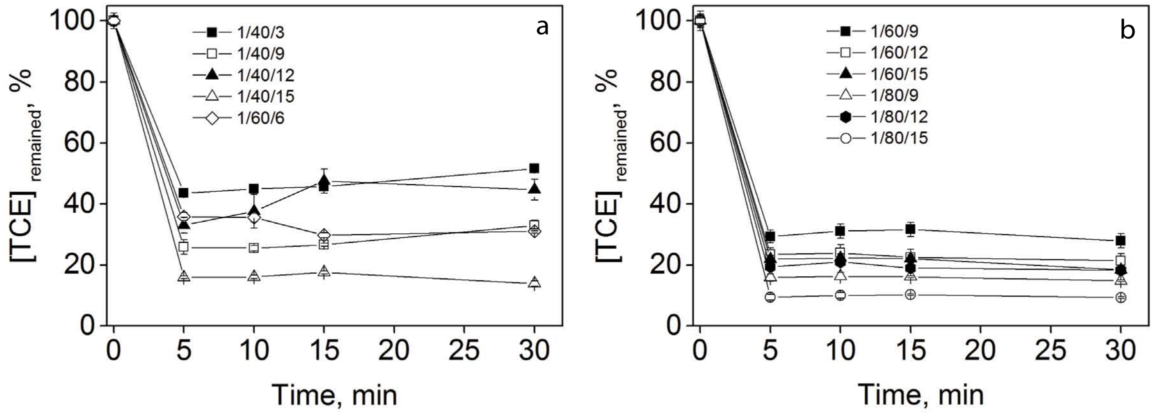

Fig. 5. Degradation of TCE by the $S_2O_8^{2-}/Fe^{2+}$ process ($TCE/S_2O_8^{2-}/Fe^{2+}$ is a molar ratio, $[TCE]_0$ = 0.228 mmol/L).

most of the iron precipitation in the Fe^{2+}/H_2O_2 process can dissolve.

3.2.3. Optimization of $Fe^{2+}/H_2O_2/S_2O_8^{2-}$ process by using RSM

3.2.3.1. Mat.hematical models and variance analysis

Based on the results obtained from the Fe^{2+}/H_2O_2 and $S_2O_8^{2-}/Fe^{2+}$ processes, the selected variation of X_1, X_2, and X_3 were 9–15, 20–60, and 40–80, respectively (Table 4).

In accordance to Box–Behnken design principles, a 3-level-3-factor of a 17 experimental points experiment was designed and the results are shown in Table 5. Y_1 and Y_2 represent TCE removal efficiency and the total remaining iron (%), respectively. As presented in Table 5, the iron loss can be controlled between 3.04% and 6.62% in the $Fe^{2+}/H_2O_2/S_2O_8^{2-}$ process in comparison with the Fe^{2+}/H_2O_2 process (14.42%–27.64%), suggesting that the $Fe^{2+}/H_2O_2/S_2O_8^{2-}$ process can achieve the goal of minimizing iron loss. The TCE removal efficiency was 74.91%–98.97%, in the $Fe^{2+}/H_2O_2/S_2O_8^{2-}$ process, compared with that of 78.96%–93.97% in Fe^{2+}/H_2O_2 process, which showed a significant advance in TCE removal. Model predictions and data analysis were analyzed by analysis of variance (ANOVA).

Table 4
Process control parameters and their limits (molar ratio)

Parameters	Notations	Limits		
		−1	0	+1
Fe^{2+}/TCE	X_1	9	12	15
H_2O_2/TCE	X_2	20	40	60
$S_2O_8^{2-}$/TCE	X_3	40	60	80

Table 5
The design matrix and the measured values (t = 30min)

No.	Process parameter			Measured value	Measured value
	X_1	X_2	X_3	Y_1 (%)	Y_2 (%)
1	−1	1	0	94.68	93.77
2	−1	0	−1	80.75	93.7
3	0	−1	1	84.00	96.52
4	0	0	0	87.80	96.72
5	1	1	0	95.01	95.38
6	0	1	−1	89.54	96.96
7	1	−1	0	84.06	94.44
8	0	−1	−1	74.91	94.02
9	0	0	0	89.19	96.37
10	−1	0	1	92.03	93.42
11	1	0	1	96.79	96.69
12	1	0	−1	87.20	96.71
13	0	0	0	88.30	96.83
14	−1	−1	0	75.51	93.99
15	0	1	1	98.97	96.96
16	0	0	0	88.26	97.52
17	0	0	0	87.17	96.01

ANOVA was performed to justify the significance and adequacy of the developed regression model. The adequacy of the model is tested using the sequential *F*-value, *p*-value, and R^2 [33], which are shown in Table 6. The *F*-value of Y_1 and Y_2 were 155.61 and 4.54, while the *p*-value of Y_1 and Y_2 was less than 0.05 (i.e., α = 0.05, or 95% confidence level), which indicated that the model results can be considered as statistically significant [33]. R^2 of Y_1 and Y_2 were 0.9950 and 0.8538, which indicated that 99.5% (Y_1) or 85.38% (Y_2) of the variability in the response can be predicted. "Adequate Precision" measured the signal to noise ratio, in which a ratio greater than 4 is desirable. The ratio of Y_1 and Y_2 were 45.038 and 6.515, indicating an adequate signal.

In accordance with the variables significant analysis from ANOVA, as shown in Table 6, X_1, X_2 and X_3 have a linear relationship with Y_1, X_1; X_2 has a significant interaction in Y_1; and X_1^2 and X_2^2 have a significant surface response in Y_1. In terms of the effects of variables in the TCE removal process, $X_2 > X_3 > X_1$. X_1 and X_2 have a linear relationship with Y_2; X_2 and X_3 has a significant interaction in Y_2; and X_1^2 and X_2^2 has a significant surface response in Y_2. The effects of variables in iron loss control processes are as follows, from greatest to least: $X_1 > X_2 > X_3$.

3.2.3.2. Optimization of $Fe^{2+}/H_2O_2/S_2O_8^{2-}$ in TCE removal and iron loss control

The main goals of the optimization process were to minimize iron loss and increase the TCE removal efficiency through reducing the usage of oxidants, especially in terms of Fe^{2+} usage. TCE removal efficiency varied from 74.91% to 98.97% during the experiment, in order to guarantee high TCE removal in the $Fe^{2+}/H_2O_2/S_2O_8^{2-}$ process, Y_1 was set from 90% to 99% in the optimization process. The remaining iron ranged from 93.42% to 96.96% to improve its quality and Y_2 was modified from 90% to 99% during the optimization.

According to the results obtained from Design Expert software, the optimum parameters with the greatest desirability are shown in Table 7. 15 recommended groups all exhibited good desirability. 5 optimized results were selected (based on the Fe^{2+} usage, from low to high) to minimize iron loss and increase TCE removal efficiency through reducing the usage of oxidants, they were: $X_1/X_2/X_3$ = 13.61/56.81/80.00, 13.33/57.33/80.00, 12.82/58.02/80.00, 14.69/53.67/80.0, and 9.00/56.63/76.25, respectively. The optimal parameters were tested to compare with the predicted results (Table 8). The results indicated that the predicted TCE removal values and remaining iron values were in good agreement with the experimental values. Therefore, the optimized process parameters obtained by the model can be used confidently.

The highest TCE removal efficiency occurred with $X_1/X_2/X_3$ = 9.00/56.63/76.25 (98.63%), the least iron loss accrued at $X_1/X_2/X_3$ = 13.61/56.81/80.00. pH varied from 3.05 to 3.12 before the reaction and down to 2.57–2.74 after the reaction (Table 8), suggesting that the five selected $Fe^{2+}/H_2O_2/S_2O_8^{2-}$ processes have the ability to drop down the pH and thus decrease the iron precipitation. The iron loss amount of $X_1/X_2/X_3$ = 13.61/56.81/80.00 was 13.61 × (100–97.93%) = 0.28, compared with the iron loss amount of $X_1/X_2/X_3$ = 9.00/56.63/76.25, which was 0.26. In accordance to the TCE removal efficiency and iron loss, the appropriate $Fe^{2+}/H_2O_2/S_2O_8^{2-}$ ratio could

Table 6
ANOVA table of Y_1 and Y_2

Source	Y_1: Sum of squares	Y_1: F value	Y_1: P value		Y_2: Sum of squares	Y_2: F value	Y_2: P value	
Model	720.56	155.61	0.00	Significant	26.97	3.91	0.04	Significant
X_1	50.45	98.05	0.00		8.69	11.34	0.01	
X_2	445.81	866.46	0.00		2.10	2.74	0.14	
X_3	193.95	376.95	0.00		0.61	0.79	0.40	
X_1X_2	16.89	32.83	0.00		0.34	0.44	0.53	
X_1X_3	0.71	1.39	0.28		0.017	0.022	0.89	
X_2X_3	0.029	0.056	0.82		1.56	2.04	0.20	
X_1^2	2.40	4.66	0.07		11.32	14.78	0.01	
X_2^2	10.55	20.51	0.00		1.81	2.36	0.17	
X_3^2	0.36	0.71	0.43		0.027	0.035	0.86	
Residual	3.60				5.36			
Lack-of-fit	1.40	0.85	0.53	Not significant	4.09	4.28	0.20	Not significant
Pure error	2.20				1.27			
Cor total	724.16				32.34			

Notes (Y_1): $R^2 = 0.9950$, Adj $R^2 = 0.9886$, Pred $R^2 = 0.9643$, Adequate precision = 45.038.
Notes (Y_2): $R^2 = 0.8341$, Adj $R^2 = 0.6208$, Pred $R^2 = -1.0856$, Adequate precision = 5.730.

Table 7
Optimization results of the experiment

No.	X_1	X_2	X_3	Y_1	Y_2	Desirability	
1	13.61	56.81	80.00	99.00	96.74	0.865	Selected
2	13.56	56.90	80.00	99.00	96.74	0.865	
3	13.69	56.64	80.00	99.00	96.74	0.865	
4	13.53	56.97	79.99	99.00	96.74	0.865	
5	13.78	56.43	80.00	99.00	96.74	0.865	
6	13.33	57.33	80.00	99.00	96.73	0.865	Selected
7	13.71	57.00	80.00	99.08	96.72	0.864	
8	14.17	55.42	80.00	99.00	96.69	0.862	
9	12.86	57.97	80.00	99.00	96.65	0.860	
10	12.82	58.02	80.00	99.00	96.65	0.859	Selected
11	13.49	59.68	80.00	99.48	96.621	0.858	
12	14.69	53.67	80.00	99.00	96.561	0.853	Selected
13	12.35	60.00	80.00	99.34	96.42	0.845	
14	14.10	51.81	80.00	98.25	96.82	0.833	
15	9.00	56.53	76.25	97.77	93.60	0.587	Selected

Table 8
Optimization results of the experiment (Predicted, P; Measured, M)

No.	X_1	X_2	X_3	P-Y_1	P-Y_2	M-Y_1	M-Y_2	Initial pH	Final pH
A	13.61	56.81	80.00	99.00	96.74	97.06	97.93	3.12	2.61
B	13.33	57.33	80.00	99.00	96.74	97.60	92.16	3.06	2.57
C	12.82	58.02	80.00	99.00	96.74	97.60	94.26	3.07	2.7
D	14.69	53.67	80.00	99.00	96.74	96.60	94.20	3.09	2.7
E	9.00	56.53	76.25	99.00	96.74	98.63	97.16	3.05	2.74

be $X_1/X_2/X_3$ = 9.00/56.63/76.25, which was where the most TCE removal occurred with the least iron loss in the reaction.

As shown in Fig. 6, there were little differences in the $HO^\bullet$ generation of five $Fe^{2+}/H_2O_2/S_2O_8^{2-}$ processes. In consideration of oxidation ability, TCE removal, iron loss, and pH control, $Fe^{2+}/H_2O_2/S_2O_8^{2-} = X_1/X_2/X_3$ = 9.00/56.63/76.25 was optimal for AC regeneration.

3.3. Evaluation of optimized $Fe^{2+}/H_2O_2/S_2O_8^{2-}$ in AC regeneration

The regeneration of AC by the optimized $Fe^{2+}/H_2O_2/S_2O_8^{2-}$ process is shown in Fig. 7. Three adsorption/regeneration cycles were conducted, the average removal efficiency of adsorbed TCE was 26.28%. A significant promotion is the adsorption capacity of AC keeps relatively stable during the three adsorption/regeneration cycles, which indicated the lifespan of AC partly prolonged through the regeneration.

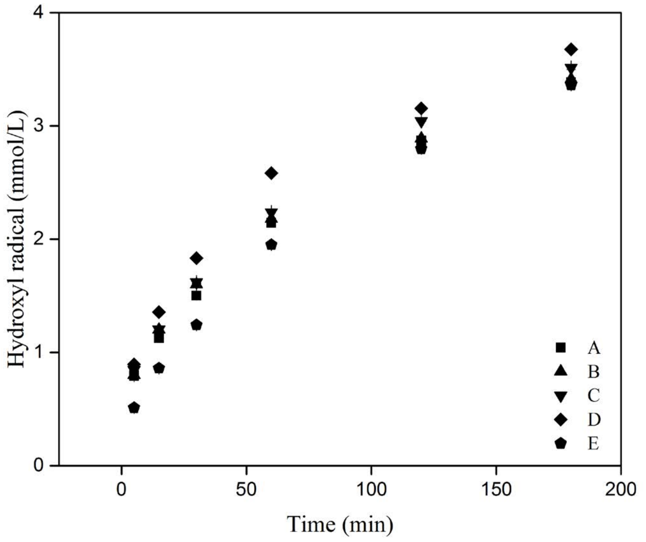

Fig. 6. $HO^\bullet$ generation in different $Fe^{2+}/H_2O_2/S_2O_8^{2-}$ process (A: $Fe^{2+}/H_2O_2/S_2O_8^{2-}/TCE$ = 13.61/56.81/80/1; B: $Fe^{2+}/H_2O_2/S_2O_8^{2-}/TCE$ = 13.33/57.33/80/1; C: $Fe^{2+}/H_2O_2/S_2O_8^{2-}/TCE$ = 12.82/58.02/80/1; D: $Fe^{2+}/H_2O_2/S_2O_8^{2-}/TCE$ = 14.69/53.67/80/1; E: $Fe^{2+}/H_2O_2/S_2O_8^{2-}/TCE$ = 9.00/56.63/76.25/1, in molar ratio. $[TCE]_0$ = 60 mg (0.458 mmol), initial pH of regeneration is 3).

Iron precipitation on the surface of AC after regeneration started to accumulate, which resulted in the decrease of AC's adsorption capacity (Figs. 8 and 9). However, compared with the initial $Fe^{2+}/H_2O_2/S_2O_8^{2-}$ process (Fig. 3), iron precipitation on AC's surface reduced significantly. From Table 9 we can see that after regeneration the iron content on AC's surface was increased from 0.32% to 2.30% in comparison with the iron content change (2.68–6.52%) in the initial $Fe^{2+}/H_2O_2/S_2O_8^{2-}$ process (Table 10). The increase meant that iron precipitation or iron oxides largely reduced on AC's surface or its pores by the optimized $Fe^{2+}/H_2O_2/S_2O_8^{2-}$ process. The other significant phenomenon was the variation of Cl content. In the optimized $Fe^{2+}/H_2O_2/S_2O_8^{2-}$ process, the amount of Cl increased from 0.14% to 0.52% (Table 9), while in the initial $Fe^{2+}/H_2O_2/S_2O_8^{2-}$ process, Cl increased from 0.18% to 2.68% (Table 10). The decrease indicates that more TCE was removed from AC by the optimized $Fe^{2+}/H_2O_2/S_2O_8^{2-}$ process. Furthermore, C loss in the optimized and initial oxidation processes showed no significant difference in values compared with the initial $Fe^{2+}/H_2O_2/S_2O_8^{2-}$ process, suggesting that the optimized $Fe^{2+}/H_2O_2/S_2O_8^{2-}$ process can avoid the extra C loss.

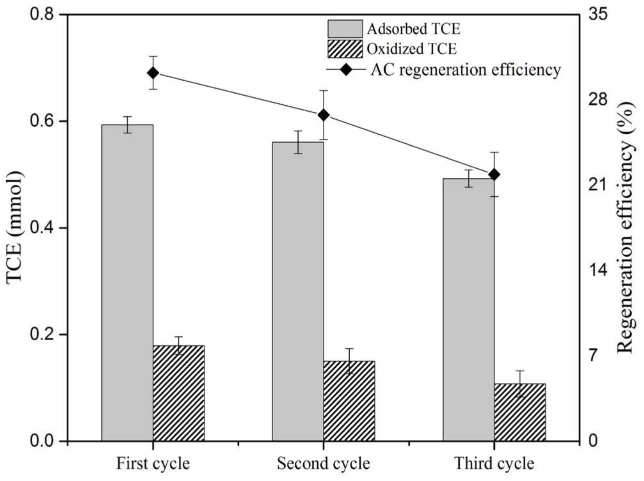

Fig. 7. AC regeneration by $Fe^{2+}/H_2O_2/S_2O_8{}^{2-}$ process (with molar ratio of $Fe^{2+}/H_2O_2/S_2O_8{}^{2-}/TCE$ = 9.00/56.63/76.25/1, $[TCE]_0$ = 60 mg (0.458 mmol), initial pH of regeneration is 3).

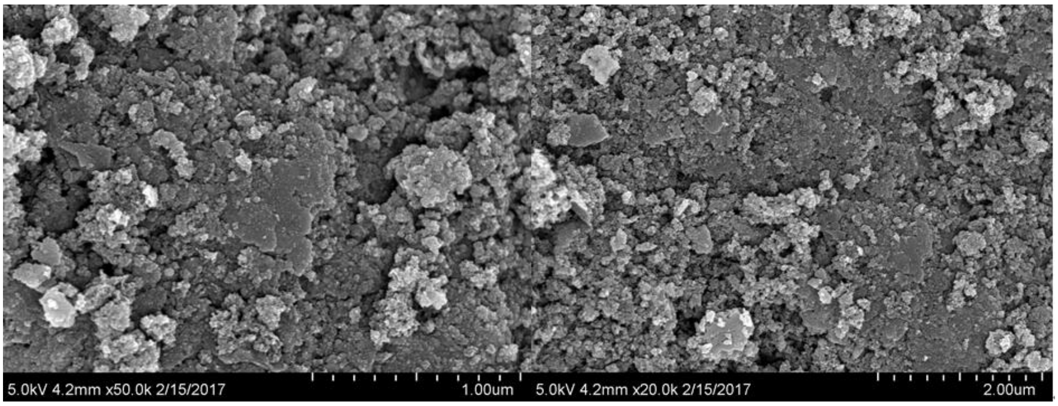

Fig. 8. AC surface before regeneration by $Fe^{2+}/H_2O_2/S_2O_8^{2-}$ process (with molar ratio of $Fe^{2+}/H_2O_2/S_2O_8^{2-}/TCE$ = 9.00/56.63/76.25/1, $[TCE]_0$ = 60 mg (0.458 mmol), initial pH of regeneration is 3).

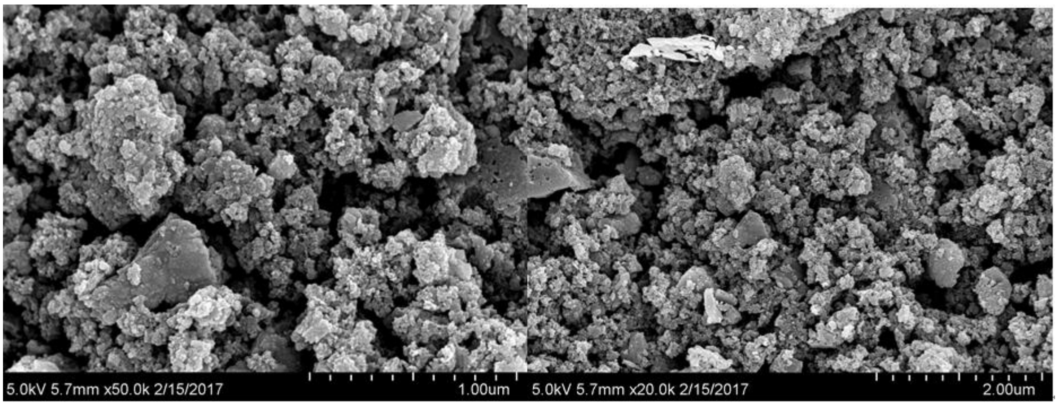

Fig. 9. AC surface after regeneration by $Fe^{2+}/H_2O_2/S_2O_8^{2-}$ process (with molar ratio of $Fe^{2+}/H_2O_2/S_2O_8^{2-}$/TCE = 9.00/56.63/76.25/1, $[TCE]_0$ = 60 mg (0.458 mmol), initial pH of regeneration is 3).

Table 9
AC surface elements change during regeneration by $Fe^{2+}/H_2O_2/S_2O_8^{2-}$ process (with molar ratio of $Fe^{2+}/H_2O_2/S_2O_8^{2-}$/TCE = 9.00/56.63/76.25/1, $[TCE]_0$ = 60 mg (0.458 mmol), initial pH of regeneration is 3)

Element	Original AC intensity (c/s)	Conc (wt.%)	Original AC intensity (c/s)	Conc (wt.%)
C	390.90	70.84	200.59	46.37
N	0.00	0.00	0.00	0.00
O	30.96	9.48	210.32	20.09
Na	3.24	0.13	9.53	0.32
Al	49.42	1.31	535.05	11.49
Si	608.48	15.57	666.56	17.69
S	17.17	0.52	1.48	0.04
Cl	4.53	0.14	0.93	0.52
Ti	15.96	0.77	7.64	0.28
Fe	3.94	0.32	38.11	2.30
P	27.95	0.91	29.09	0.90

Table 10
AC surface elements change during regeneration by $Fe^{2+}/H_2O_2/S_2O_8^{2-}$ process (with molar ratio of $Fe^{2+}/H_2O_2/S_2O_8{}^{2-}$/TCE = 0.5/20/1/1, $[TCE]_0$ = 60 mg (0.458 mmol), initial pH of regeneration is 3)

Element	Original AC intensity (c/s)	Conc (wt.%)	Regenerated AC intensity (c/s)	Conc (wt.%)
C	349.36	81.88	129.00	55.69
N	0.77	2.17	0.00	0.00
O	12.58	9.43	48.49	22.36
Na	1.61	0.23	0.61	0.09
Al	5.85	0.59	5.62	0.55
Si	18.98	1.85	0.00	0.00
S	16.02	1.68	10.47	1.08
Cl	1.50	0.18	23.91	2.68
Ti	0.00	0.000	4.00	0.71
Fe	2.70	0.99	19.67	6.52
P	0.00	0.00	19.47	2.03

As with AC's surface area and pore volume, BET surface area of the optimized $Fe^{2+}/H_2O_2/S_2O_8^{2-}$ process decreased 31.29% (Table 11), which was less than the 43.9% of the initial $Fe^{2+}/H_2O_2/S_2O_8^{2-}$ process (Table 1). The total area in pores ≥0.47 nm decreased to 61.3% in the initial $Fe^{2+}/H_2O_2/S_2O_8^{2-}$ process (Table 1), a value that was much higher than the optimized $Fe^{2+}/H_2O_2/S_2O_8^{2-}$ process (50.19%, Table 1). The aforementioned values suggest that compared with the initial $Fe^{2+}/H_2O_2/S_2O_8^{2-}$ process, the optimized $Fe^{2+}/H_2O_2/S_2O_8^{2-}$ process possessed a better application prospect.

Table 11
Change of AC's surface area by $Fe^{2+}/H_2O_2/S_2O_8^{2-}$ process (with molar ratio of $Fe^{2+}/H_2O_2/S_2O_8^{2-}/TCE$ = 9.00/56.63/76.25/1, $[TCE]_0$ = 60 mg (0.458 mmol), initial pH of regeneration is 3)

Category	Original AC	Regenerated AC
BET surface area (m²/g)	637.41	437.99
Volume in pores <0.486 nm (cm³/g)	0	0.02
Total volume in pores ≤44.883 nm (cm³/g)	0.64	0.48
Total area in pores ≥0.486 nm (m²/g)	1,784.64	889.02

It can be concluded that the optimized $Fe^{2+}/H_2O_2/S_2O_8^{2-}$ process can regenerate AC effectively with less iron loss, high TCE removal, and destroy less of AC's surface. Although the surface area and pore volume of AC was affected by iron precipitation and oxidants during the regeneration process, the adsorption capacity of AC can support long-term use.

4. Conclusion

The optimization of $Fe^{2+}/H_2O_2/S_2O_8^{2-}$ using RSM showed that with the molar ratio of $TCE/Fe^{2+}/H_2O_2/S_2O_8^{2-}$ of 1/9.00/56.63/76.25, the predicted TCE removal values (98.63%) are in agreement with the experimental values (99.00%). Furthermore, the iron loss obtained from the test was 2.84%, suggesting that the goals of minimizing iron loss and reducing the usage amount of oxidants on the basis of high TCE removal were achieved by RSM. The regeneration rate of AC by optimized $Fe^{2+}/H_2O_2/S_2O_8^{2-}$ was 26.28% on average in three adsorption/oxidation cycles and the surface area and pore volume of AC were reduced during the regeneration, however, the long-term use of AC was achieved.

Acknowledgment

This work was financially supported by National Natural Science Foundation of China (NSFC) (41272268); the Special Fund for Public Interest research was supported by the Ministry of Environmental Protection (201309001-3); and the project of application and demonstration of groundwater dating technologies in Hebei plain (201511046-4).

References

[1] J.W. Park, S.S. Lee, D.K. Choi, Y.W. Lee, Y.M. Kim, Adsorption equilibria of toluene, dichloromethane, and trichloroethylene onto activated carbon fiber, J. Chem. Eng. Data, 47 (2002) 980–983.

[2] L.C. Toledo, A.C.B. Silva, R. Augusti, R.M. Lago, Application of Fenton's reagent to regenerate activated carbon saturated with organochloro compounds, Chemosphere, 50 (2003) 1049–1054.

[3] A. Cabrera-Codony, R. Gonzalez-Olmos, M.J. Martín, Regeneration of siloxane-exhausted activated carbon by advanced oxidation processes, J. Hazard. Mater., 285 (2015) 501–508.

[4] S.G. Huling, E. Kan, C. Caldwell, S. Park, Fenton-driven chemical regeneration of MTBE-spent granular activated carbon – a pilot study, J. Hazard. Mater., 205–206 (2012) 55–62.

[5] C. Liang, Y.T. Lin, W.H. Shin, Persulfate regeneration of trichloroethylene spent activated carbon, J. Hazard. Mater., 168 (2009) 187–192.

[6] S. Ko, M. Crimi, B.K. Marvin, V. Holmes, S.G. Huling, Comparative study on oxidative treatments of NAPL containing chlorinated ethanes and ethenes using hydrogen peroxide and persulfate in soils, J. Environ. Manage., 108 (2012) 42–48.

[7] J. Zhao, J. Yang, J. Ma, Mn(II)-enhanced oxidation of benzoic acid by Fe(III)/H_2O_2 system, Chem. Eng. J., 239 (2014) 171–177.

[8] I. Innocenti, I. Verginelli, F. Massetti, D. Piscitelli, R. Gavasci, R. Baciocchi, Pilot-scale ISCO treatment of a MtBE contaminated site using a Fenton-like process, Sci. Total Environ., 485–486 (2014) 726–738.

[9] K.-C. Huang, R.A. Couttenye, G.E. Hoag, Kinetics of heat-assisted persulfate oxidation of methyl tert-butyl ether (MTBE), Chemosphere, 49 (2002) 413–420.

[10] M. Usman, P. Faure, K. Hanna, M. Abdelmoula, C. Ruby, Application of magnetite catalyzed chemical oxidation (Fenton-like and persulfate) for the remediation of oil hydrocarbon contamination, Fuel, 96 (2012) 270–276.

[11] J. Sahl, J. Munakata-Marr, The effects of in situ chemical oxidation on microbiological processes: a review, Remediation J., 16 (2006) 57–70.

[12] C. Sirguey, P.T.S. e Silva, C. Schwartz, M.-O. Simonnot, Impact of chemical oxidation on soil quality, Chemosphere, 72 (2008) 282–289.

[13] W. Chu, Y.R. Wang, H.F. Leung, Synergy of sulfate and hydroxyl radicals in UV/$S_2O_8^{2-}$/H_2O_2 oxidation of iodinated X-ray contrast medium iopromide, Chem. Eng. J., 178 (2011) 154–160.

[14] C. Liang, M.-C. Lai, Trichloroethylene degradation by zero valent iron activated persulfate oxidation, Environ. Eng. Sci., 25 (2008) 1071–1077.

[15] C. Liang, Y.-Y. Guo, Y.-C. Chien, Y.-J. Wu, Oxidative degradation of MTBE by pyrite-activated persulfate: proposed reaction pathways, Ind. Eng. Chem. Res., 49 (2010) 8858–8864.

[16] X.-R. Xu, X.-Y. Li, X.-Z. Li, H.-B. Li, Degradation of melatonin by UV, UV/H_2O_2, Fe^{2+}/H_2O_2 and UV/Fe^{2+}/H_2O_2 processes, Sep. Purif. Technol., 68 (2009) 261–266.

[17] Y. Rao, L. Qu, H. Yang, W. Chu, Degradation of carbamazepine by Fe (II)-activated persulfate process, J. Hazard. Mater., 268 (2014) 23–32.

[18] C. Liang, Z.-S. Wang, C.J. Bruell, Influence of pH on persulfate oxidation of TCE at ambient temperatures, Chemosphere, 66 (2007) 106–113.

[19] A. Ghauch, G. Ayoub, S. Naim, Degradation of sulfamethoxazole by persulfate assisted micrometric Fe^0 in aqueous solution, Chem. Eng. J., 228 (2013) 1168–1181.

[20] C. Liang, C.J. Bruell, M.C. Marley, K.L. Sperry, Persulfate oxidation for in situ remediation of TCE. I. Activated by ferrous ion with and without a persulfate–thiosulfate redox couple, Chemosphere, 55 (2004) 1213–1223.

[21] C. Liang, C.-F. Huang, N. Mohanty, C.-J. Lu, R.M. Kurakalva, Hydroxypropyl-β-cyclodextrin-mediated iron-activated persulfate oxidation of trichloroethylene and tetrachloroethylene, Ind. Eng. Chem. Res., 46 (2007) 6466–6479.

[22] N. Yan, F. Liu, W. Huang, Interaction of oxidants in siderite catalyzed hydrogen peroxide and persulfate system using trichloroethylene as a target contaminant, Chem. Eng. J., 219 (2013) 149–154.

[23] P.A. Block, R.A. Brown, D. Robinson, Novel Activation Technologies for Sodium Persulfate In Situ Chemical Oxidation, in: Proc. Fourth International Conference on the Remediation of Chlorinated and Recalcitrant Compounds, 2004.

[24] N. Dulova, E. Kattel, M. Trapido, Degradation of naproxen by ferrous ion-activated hydrogen peroxide, persulfate and combined hydrogen peroxide/persulfate processes: the effect of citric acid addition, Chem. Eng. J., 318 (2016) 254–263.

[25] D.C. Montgomery, Design and Analysis of Experiments, Wiley, New York, 1984.

[26] W. Wang, Y. Xiao, X. Wu, J. Zhang, Optimization of laser-assisted glass frit bonding process by response surface methodology, Optics Laser Technol., 77 (2016) 111–115.

[27] S.A. Heleno, P. Diz, M. Prieto, L. Barros, A. Rodrigues, M.F. Barreiro, I.C. Ferreira, Optimization of ultrasound-assisted extraction to obtain mycosterols from *Agaricus bisporus* L. by response surface methodology and comparison with

conventional Soxhlet extraction, Food Chem., 197 (2016) 1054–1063.

[28] D.B. Mawhinney, R.B. Young, B.J. Vanderford, T. Borch, S.A. Snyder, Artificial sweetener sucralose in U.S. drinking water systems, Environ. Sci. Technol., 45 (2011) 8716–8722.

[29] M.E. Lindsey, M.A. Tarr, Quantitation of hydroxyl radical during Fenton oxidation following a single addition of iron and peroxide, Chemosphere, 41 (2000) 409–417.

[30] W.R. Haag, C.D. Yao, Rate constants for reaction of hydroxyl radicals with several drinking water contaminants, Environ. Sci. Technol., 26 (1992) 1005–1013.

[31] C. Moreno-Castilla, Adsorption of organic molecules from aqueous solutions on carbon materials, Carbon, 42 (2004) 83–94.

[32] J.S. Mattson, H.B. Mark, Activated Carbon: Surface Chemistry and Adsorption from Solution, M. Dekker, New York, 1971.

[33] B. Acherjee, D. Misra, D. Bose, K. Venkadeshwaran, Prediction of weld strength and seam width for laser transmission welding of thermoplastic using response surface methodology, Optics Laser Technol., 41 (2009) 956–967.